J. Phys. Chem. A **2004,** *108,* 7331−7338

Hydrogen Bonding in ROH:R′OH (R, R′ = H, CH_3, C_2H_5) Heterodimers: Matrix-Dependent Structure and Infrared-Induced Isomerization

S. Coussan,[†] P. Roubin,[†] and J. P. Perchard*,[‡]

Laboratoire PIIM, UMR 6633, Equipe SDM, Service 242, Université de Provence, CNRS,
Centre Saint-Jérôme, 13397 Marseille Cedex 20, France, and Laboratoire de Dynamique,
Interactions et Réactivité, CNRS UMR 7075, Université Pierre et Marie Curie,
Bâtiment F 74, case courrier 49, 4 Place Jussieu, 75252 Paris Cedex 05, France

Received: April 19, 2004; In Final Form: June 15, 2004

The structure of ROH:R′OH heterodimers (R, R′ = H, CH_3, C_2H_5) trapped in argon and nitrogen matrixes was examined through two approaches: $^{16}O/^{18}O$ isotopic substitution in water and methanol and infrared-induced isomerization. Isotopic substitution clearly shows that in N_2 matrix the bigger molecule plays the role of proton donor (Type-I structure) and in Ar matrix that of proton acceptor (Type-II structure). This difference can be rationalized by considering the existence of weak $OH\cdots N_2$ hydrogen bonds stabilizing the less stable structure. Selective irradiations in the νOH region were carried out for the CH_3OH:H_2O and C_2H_5OH:H_2O dimers. Type-I → Type-II interconversion was observed in N_2 matrix while no effect was detected in Ar. Finally the hydrogen bond strength evolution within the nine ROH:R′OH homo- and heterodimers was examined on both experimental and theoretical grounds. Experimentally this evolution was followed by considering the νOH frequency shifts of the proton donor subunit. Theoretically ab initio calculations of the structures, energies, and harmonic frequencies were performed in the DFT approach. In both cases for a given proton donor the frequency shift with respect to the monomer increases with the basicity of the proton acceptor (i.e. in the order $H_2O < CH_3OH < C_2H_5OH$); similarly, for a given proton acceptor, it increases with the acidity of the hydroxyl group (i.e. in the order $C_2H_5OH < CH_3OH < H_2O$). One exception, the C_2H_5OH:CH_3OH Type-I heterodimer, for which the νOH shift of ethanol does not follow these rules, is experimentally observed. On the other hand the calculated dissociation energies and $O\cdots O$ distances also correctly vary according to the basicity of the proton acceptor and the acidity of the proton donor.

I. Introduction

Infrared photodepletion spectroscopy coupled to molecular beams proved to be the most powerful tool for studying small aggregates, especially those involving hydrogen bonding. It does not require the presence of species with low energy excited electronic states nor fluorescent molecules and has been successfully applied to simple but important systems such as water and methanol polymers, with aggregation states up to decamer. A review on these systems has been recently published by Buck and Huisken.[1] From the comparison between size-selected depletion spectra in the 3 μm region and calculated ones, structural information is deduced. On the other hand it has been shown that IR photochemistry in inert matrices can be a useful complementary technique despite a lack of size selectivity limiting the spectral analysis to low states of polymerization which, up to now, cannot exceed the tetramer because of spectral congestion. A subsidiary interest of selective infrared irradiation in matrix lies in the possibility of recombination of the fragments of photolysis, giving rise to high energy isomers stabilized by the sterical constraints of the surroundings. This property will be considered in the present paper devoted to the study of the ROH:R′OH (R, R′ = H, CH_3, C_2H_5) heterodimers trapped in argon and nitrogen, which can exist under two different forms by reversing the role of proton acceptor (PA) and proton donor (PD) of the two partners. In what follows, these structures will be referred to as Type-I and Type-II according to whether the smaller acts as PA or PD, respectively. For R = H and R′ = CH_3, Type-II only has been identified in the gas phase[2,3] and in argon matrix[4] while Type-I has been characterized in solid nitrogen.[5] The purpose of the present work, in the continuity of previous studies on the photoisomerization of heterodimers containing either methanol[6,7] or water,[8] is to examine the possibility of Type-I ⇄ Type-II interconversion processes induced by selective excitation of OH stretching vibrations in the 2.8 μm region. For the heterodimers involving ethanol, which can exist under two conformations, anti and gauche, previous studies[9−11] on C_2H_5OH monomer and dimer trapped in Ar and N_2 matrices will be used as a basis for identifying its conformation and its donor/acceptor character.

II. Experimental Section

Samples were prepared in a closed cycle helium cryostat (Cryomech PT-405) by fast deposition of gas mixtures on a Au-plated Cu block. The deposition rate was 250 mmol/h, and the deposition temperature was 16 (N_2 matrix) or 19 K (Ar matrix). Samples were studied in the 4−20 K temperature range, using a Bruker IFS/66S interferometer with a resolution of 0.13 cm^{-1}.

---

* To whom correspondence should be addressed. E-mail: jpp@spmol.jussieu.fr.

[†] Université de Provence.

[‡] Université Pierre et Marie Curie.

10.1021/jp048303t CCC: \$27.50

TABLE 1: Dissociation Energies[a] (kcal mol^{-1}) and O···O Distances (Å) (in parentheses) Calculated for the ROH−R′OH Dimers (R, R′ = H, CH$_3$, C$_2$H$_5$)

PA/PD		H$_2$O	CH$_3$OH	C$_2$H$_5$OH	
				A	G
H$_2$O		4.6−2.4 (2.919)[b]	4.3−2.7 (2.930)	4.1−2.6 (2.947)	4.1−2.6 (2.942)
CH$_3$OH		4.9−3.0 (2.885)	4.7−3.3 (2.893)	4.5−3.1 (2.900)	4.4−3.1 (2.907)
C$_2$H$_5$OH	A	5.0−3.0 (2.886)	4.7−3.4 (2.893)	4.6−3.3 (2.900)[c]	4.4−3.1 (2.912)[c]
	G	5.0−3.2 (2.885)	4.8−3.5 (2.892)	4.7−3.5 (2.887)[c]	4.6−3.4 (2.897)[c]

[a] D_e values, after BSSE correction (left) and D_0 values, after BSSE and ZPE corrections (right). [b] Reference 12. [c] Reference 10.

TABLE 2: Frequency Shifts[a] (cm^{-1}) and Relative Band Intensities (in parentheses) of Water Engaged in Heterodimers with Methanol and Ethanol. Comparison between Calculated Harmonic and Observed Values in N$_2$ Matrix

		CH$_3$OH:H$_2$O				C$_2$H$_5$OH:H$_2$O			
	monomer	PD (Type-II dimer)		PA (Type-I dimer)		PD (Type-II dimer)		PA (Type-I dimer)	
	calcd[b]	calcd	obsd (N$_2$)	calc	obsd[c] (N$_2$, δ)	calcd (gauche)	obsd (N$_2$)	calc (anti)	obsd (N$_2$)
ν_3	3923.1	−31.1 (20)	−27.7 (48)	−10.8 (20)	−14.3 (44)	−31.0 (19)	−27.0 (29)	−11.5 (25)	−12.7 (34)
ν_1	3821.2	−157.0 (100)	−110.9 (100)	−6.6 (2.9)	−7.7 (6.0)	−152.3 (100)	−134.4 (100)	−7.7 (3.0)	−3.8 (3.8)
ν_2	1639.4	21.8 (11)	22.7 (26)	4.0 (19)	6.0 (24)	22.8 (8.8)	27.3 (13)	3.9 (22)	6.4 (15)

[a] $\Delta\nu = \nu_{\mathrm{dimer}} - \nu_{\mathrm{monomer}}$. [b] Reference 12. [c] Reference 5.

TABLE 3: Frequency Shifts[a] (cm^{-1}) and Relative Band Intensities (in parentheses) of Methanol Engaged in Heterodimers with Water and Ethanol. Comparison between Calculated (harmonic) and Observed Values in N$_2$ or Ar Matrix

		CH$_3$OH:H$_2$O				CH$_3$OH:C$_2$H$_5$OH			
	monomer	PD (Type-I dimer)		PA (Type-II dimer)		PD (Type-II dimer)		PA (Type-I dimer)	
	calcd	calcd	obsd (N$_2$, δ)	calcd	obsd(N$_2$)	calcd (Anti)	obsd (Ar)[a]	calcd (Anti)	obsd (N$_2$)
νOH	3851.4	−124.0 (100)	−132.3 (100)	−7.0 (11)	−2.7 (42)	−166.1 (100)	−151 (100)	−6.4 (8.1)	−9.0 (24)
ν_sCH$_3$	3003.0	−11.6 (19)	−7.4 (12)	21.3 (12)	4.0 (8.5)	−13.8 (16)	−10.5	20.8 (6.7)	−7.7 (5.5)
δOH	1371.2	49.3 (11)	44.1 (8.0)	0.1 (6.8)	2.9 (17)	61.8 (6.9)		0.0 (4.3)	
νCO	1037.4	17.8 (26)	13.6 (32)	−9.4 (29)	0.7 (46)	19.1 (21)	13.6	10.1 (27)	−4.8 (28)

[a] Mean frequency. $\Delta\nu = \nu_{\mathrm{dimer}} - \nu_{\mathrm{monomer}}$.

Irradiations were performed using an optical parametric oscillator BM-Industry, Thalès, at sample temperature of 4.0 ± 0.1 K. The line width was below 5 cm^{-1}, and the average beam power near 2.8 μm was 2 mW at the matrix sample position. Unfortunately the LiNbO$_3$ crystal contained in the master oscillator was hydrated, preventing emission in the range 3510−3460 cm^{-1}.

Natural water, methanol, and ethanol (Prolabo RP grade) were degassed under vacuum before use. H$_2{}^{18}$O (98% ^{18}O, from YEDA, Rehovoth, israël), CH$_3{}^{18}$OH (isotec, 97% ^{18}O enriched), N$_2$, and Ar (L′Air Liquide, 99.999% purity) were used without purification.

III. Theoretical Calculations

Following the procedure successfully used for the water,[12] methanol,[13] and ethanol[10] homodimers, density functional calculations on the heterodimers were carried out using the Gaussian 98/DFT series of programs[14] and the 6-311++G(2d, 2p) basis set. The DFT program uses the Becke's three-parameter functional[15] with the gradient-dependent exchange correction and the nonlocal correlation functional of Lee, Yang, and Parr.[16] For CH$_3$OH:H$_2$O, full-geometry optimizations were performed for two minima, as established by the absence of any imaginary vibrational frequency, corresponding to Type-I and Type-II structures. For the heterodimers involving ethanol which has two stable forms, anti and gauche,[9,11] four minima were examined corresponding to Type-I and Type-II structures with ethanol existing under either one or the other form. The dissociation energies (D_c) (BSSE corrected[17]) and their zero-point energy corrected values (D_0) reported in Table 1 together with the O···O distances arouse the following comments. First, Type-II heterodimers are more stable than Type-I; this is in agreement with the only observation of Type-II species in inert Ar matrix[4] and in the gas phase.[2,3] Second, examination of each column shows that the basicity increase of PA from water to methanol causes noticeable increase of the dissociation energies and a decrease of the O···O distances while the corresponding variations from methanol to ethanol are not significant. Third, on each line, the acidity decrease of PD from water to ethanol induces an increase of the O···O distances and a decrease of D_e but no satisfactory evolution of D_0 probably because of inaccurate values of the harmonic frequencies of the intermolecular modes. Comparable trends were previously reported by Mó et al[18−20] and Peeters et al.[21] On the other hand the harmonic vibrational frequencies of the heterodimers have been summarized in Tables 2−5, each of them reporting the most significant modes of one ROH molecule acting either as PA or PD (R = H, CH$_3$, C$_2$H$_5$ respectively in Tables 2, 3, 4 and 5). For an easier comparison with the experimental data, to be developed later, the frequency shifts $\Delta\nu = \nu_{\mathrm{dimer}} - \nu_{\mathrm{monomer}}$ have been reported together with the corresponding monomer frequencies.

IV. Spectral and Structural Properties of the Heterodimers

The vibrational properties of the three heterodimers in N$_2$ and Ar matrices are reported for the natural molecules and their CH$_3{}^{18}$OH:H$_2$O, C$_2$H$_5$OH:H$_2{}^{18}$O and C$_2$H$_5$OH:CH$_3{}^{18}$OH isotopomers. From the ^{16}O/^{18}O isotopic shifts of the OH stretching modes, the PA or PD character of each partner is easily deduced.

IV.A. The CH$_3$OH:H$_2$O Dimer. In solid N$_2$ the CH$_3{}^{16}$OH:H$_2$O dimer has been identified[5] in four sites labeled α, β, γ, δ, with frequencies typical of Type-I structure (Table 6). δ

TABLE 4: Frequency Shifts[a] (cm^{-1}) and Relative Band Intensities (in parentheses) of Anti Ethanol Engaged in Heterodimers with Water and Methanol. Comparison between Calculated (harmonic) and Observed Values in N_2 or Ar Matrices

		anti ethanol:H_2O				anti ethanol:CH_3OH		
	monomer	PD (Type-I dimer)		PA (Type-II dimer)		PD (Type-I dimer)	PA (Type-II dimer)	
	calcd[b]	calcd	obsd (N_2)	calcd	obsd (Ar)	calcd	calcd	obsd (Ar)
νOH	3847.1	−122.9 (100)	−125.9 (100)	−7.6 (10)	−4.9 (3.8)	−153.9 (100)	−6.4 (8.0)	−11.7
δOH	1270.5	56.4 (18)	60.6 (9.4)	5.7 (18)		55.4 (16)	6.1 (15)	
$rCH_3+\nu_aCCO$	1095.7	17.0 (5.5)	12.8 (5.8)	−9.3 (3.5)	−8.0	17.1 (4.4)	−9.3 (2.7)	−8.0
$\nu_aCO+rCH_3$	1029.3	20.7 (16)	22.5 (9.1)	6.4 (21)	3.1 (20)	21.4 (10)	5.9 (19)	3.7
ν_sCCO	894.4	4.0 (2.6)	8.8 (1.9)	−5.7 (5.1)	−1.7 (6.8)	3.8 (2.1)	−6.1 (4.6)	−4.4

[a] $\Delta\nu = \nu_{dimer} - \nu_{monomer}$. [b] Reference 9.

TABLE 5: Frequency Shifts[a] (cm^{-1}) and Relative Band Intensities (in parentheses) of Gauche Ethanol Engaged in Heterodimers with Water and Methanol. Comparison between Calculated and Observed Values

		gauche ethanol:H_2O			gauche ethanol: CH_3OH		
	monomer	PD (Type-I dimer)	PA (Type-II dimer)		PD (Type-I dimer)		PA(Type-II dimer)
	calcd	calcd	calcd	obsd (N_2)	calcd	obsd (N_2)	calcd
νOH	3832.6	−116.5 (100)	−6.7 (7.0)	−7.9 (15)	−145.3 (100)	−167.2 (100)	−6.3 (5.7)
$\delta_sCH_3+wCH_2$	1419.3	15.4 (14)	5.6 (8.1)	4.9 (7.7)	19.8 (11)	29.2 (15)	5.5 (9.7)
δOH	1282.6	15.8 (3.0)	−0.1 (2.7)		17.2 (2.0)	13.6 (1.6)	0.8 (2.2)
$\nu CCO+\delta OH$	1068.2	33.6 (21)	4.0 (17)	3.7 (9.8)	36.2 (16)	21.6 (16)	5.5 (13)
$\nu_aCCO+rCH_3$	1055.9	5.6 (15)	−4.4 (14)	−0.3 (21)	5.4 (11)		−5.4 (21)
ν_sCCO	880.8	2.8 (3.0)	1.0 (4.7)	−0.5 (3.8)	2.8 (2.2)	1.4 (1.9)	1.2 (4.2)
rCH_2+rCH_3	806.6	0.6 (1.0)	0.2 (0.6)	−2.8 (0.4)	0.9 (0.5)		3.1 (0.5)

[a] $\Delta\nu = \nu_{dimer} - \nu_{monomer}$.

TABLE 6: Comparison of Frequencies (cm^{-1}) of Some Modes[a] of the $CH_3{}^{16}OH:H_2O$ and $CH_3{}^{18}OH:H_2O$ Dimers Trapped in N_2 and Ar Matrices

	N_2 matrix[b]				Ar matrix[c]	
modes[a]	α	β	γ	δ		
ν_3						
^{16}O			3714.3	3713.2	3703.7	
^{18}O			3714.4	3713.0	3704.0	
ν_1						
^{16}O	3626.5	3627.5	3628.5	3627.2	3542.2	3535.2
^{18}O	3626.4		3628.3	3627.0	3541.5	3535.1
ν_2						
^{16}O	1599.0	1599.6	1601.9	1603.1	1613.5	
^{18}O			1602.0	1603.1	1613.8	
νOH						
^{16}O	3541.4	3536.5	3534.8	3531.6	3663.4	3662.7
^{18}O	3530.4	3525.4	3523.6	3520.3	3652.1	
νCO						
^{16}O	1048.9	1048.4	1048.0	1048.1	1032.4	1030.9
^{18}O			1020.6	1020.8	1005.5	1003.8

[a] ν_1, ν_2, ν_3 refer to the vibrational modes of $H_2{}^{16}O$. [b] Four trapping sites labeled α, β, γ, δ. δ predominates above 12 K, γ predominates at low temperature and after long exposure in the beam of the spectrometer. For ^{16}O values taken from ref 5. [c] Two trapping sites, the main one corresponding to the first column. For ^{16}O values taken from ref 4.

predominates above 10 K and is converted into γ upon exposure to the light beam of the spectrometer at low temperature. Upon $CH_3{}^{16}OH/CH_3{}^{18}OH$ isotopic substitution, the Type-I structure is confirmed by a 11 cm^{-1} red shift for the bonded OH oscillator, the frequencies of the bands assignable to water acting as PA[22,23] remaining unchanged. It is worth noting that irradiation by the source of the spectrometer induces not only the $\delta \rightarrow \gamma$ conversion[5] but also the appearance of weak features which progressively disappear when the sample is kept in the dark for some tens of minutes. The most significant are located at 3700, 3661, 3524, 2848, 1345, and 1035 cm^{-1} ($CH_3{}^{16}OH$). Their origin will be discussed in the photochemistry section.

In solid Ar the frequency of the bonded OH oscillator remains unchanged around 3540 cm^{-1} when replacing $CH_3{}^{16}OH$ by $CH_3{}^{18}OH$ while the ca. 11 cm^{-1} isotopic shift of νOH is observed between the bands at 3663 (^{16}O) and 3652 cm^{-1} (^{18}O) assignable to methanol acting as proton acceptor. Thus type-II structure in argon matrix is well confirmed by this isotopic substitution experiment.

IV.B. The $C_2H_5OH:H_2O$ Dimer. In N_2 matrix the $C_2H_5OH:H_2O$ dimer is characterized in the νOH region by three bands at 3715.0, 3631.1, and 3527.1 ($H_2{}^{16}O$) or 3700.6, 3623.8, and 3526.6 cm^{-1} ($H_2{}^{18}O$) (Table 7). The invariant frequency of the bonded OH oscillator, 3527 cm^{-1}, in the isotopic substitution demonstrates a type-I structure for this dimer, i.e., ethanol acting as PD. This conclusion agrees with the $^{16}O/^{18}O$ isotopic shifts ($\Delta\nu_3$, $\Delta\nu_1$, $\Delta\nu_2$) of the three water modes, respectively equal to 14.4, 7.3, and 6.1 cm^{-1}, close to those of the proton acceptor molecule of $(H_2O)_2$ trapped in nitrogen (14.3, 7.2 and 6.4 cm^{-1}, respectively).[22,23] As mentioned for $CH_3OH:H_2O$, prolonged exposure in the infrared beam of the spectrometer induces a significant decrease of the bands of the type-I heterodimer with concomitant appearance of bands at 3701, 3645, 3500, 1394, 1067, 1058 ($H_2{}^{16}O$) and 3688, 3645, 3491 cm^{-1} ($H_2{}^{18}O$). Their origin will be discussed in the photochemistry section.

In argon matrix, annealing of samples with H_2O/C_2H_5OH molar ratio of about 3 and $H_2O/Ar \sim 0.004$ leads to intensity increase of bands assignable either to $(H_2O)_2$[24,25] or to $C_2H_5OH:H_2O$. For this heterodimer, the three bands of water, identified by their $^{16}O/^{18}O$ isotopic shifts (Table 7), are typical of a PD molecule, the νOH mode of ethanol being located at 3650.7 cm^{-1} for both isotopomers. One thus unambiguously concludes that in argon the $C_2H_5OH:H_2O$ dimer has a type-II structure, ethanol acting as PA.

IV.C. The $C_2H_5OH:CH_3OH$ Dimer. The spectral analysis is rendered intricate by the simultaneous presence of homo- and heterodimers occupying multiple trapping sites and absorbing in the same spectral domains. As a consequence only a partial identification of the heterodimer can be obtained.

In N_2 matrix Figure 1 clearly shows that in the OH-bonded stretching region the strong band at 3482 cm^{-1} assignable to this dimer is invariant in the $^{16}O/^{18}O$ substitution, which

TABLE 7: Vibrational Frequencies (cm^{-1}) and Relative Band Intensities (in parentheses) of Type-I and Type-II C_2H_5OH:$H_2{}^{16}O$ and C_2H_5OH:$H_2{}^{18}O$ Dimers Trapped in N_2 (I and II) and Ar (II)

	Type-I[b]		Type-II		
			N_2[d]	Ar	
modes[a]	^{16}O	^{18}O	^{16}O	^{16}O	^{18}O
ν_3	3715.0 (34)	3700.6	3700.5 (29)	3705.0 (32)	3694.6
ν_1	3631.1 (3.8)	3623.8	3500.5 (100)	3534.4 (100)	3525.3 (100)
ν_2	1603.5 (15)	~1597[c]	1624.4 (13)	1614.5 (22)	1608.4 (17)
νOH	3527.1 (100)	3526.6	3645.0 (15)	3650.7 (3.8)	3650.7
νCH_3	2983.6 (7.8)		2989.2 (10)		
	2950.1 (0.9)		2956.6 (2.8)		
	2938.4 (1.5) br		2943.8 (1.5)		
	2892 (3.4) br		2904.6 (1.5)		
δCH_2	1489.4 (0.4)	1489.4	1482.6 (0.3)		
δCH_3	1459.4 (0.6)	1459.2	1456.5 (0.6)		
	1446.2 (1.2)	1446.1	1451.5 (1.8)		
twCH_2+ δCOH			1394.2 (7.7)		
	1371.6 (1.2)	1371.5	1374.0 (0.6)		
	1326.6 (1.1)	1326.3	1346.2 (1.3)		
wCH_2+ δCOH	1316.9 (9.4)	1316.9		1270 (8) br	1275 br
	1151.6 (1.4) br				
rCH_3+ν_aCCO	1103.5 (5.8)	1103.3	1067.4 (9.8)	1083.7[e]	1083.6[e]
ν_aCCO+rCH_3	1050.2 (9.1)	1050.0	1057.8 (21.5)	1028.7 (20)	1028.6 (27)
ν_sCCO	896.4 (1.9)	896.4	884.4 (3.8)	884.7 (6.8)	884.7 (7.4)
rCH_2+rCH_3	813.9 (0.3)	813.0	809.3 (0.4)		

[a] ν_1, ν_2, ν_3 refer to the water vibrational modes. [b] br = broad. [c] Overlap with the ν_2 band of $H_2{}^{16}O$ monomer makes this frequency inaccurate. [d] In N_2 the intensity ratio of the Type-II/Type-I references is $I_{3500}/I_{3527} = 0.64$. [e] Overlap with a monomer band makes intensity measurements inaccurate.

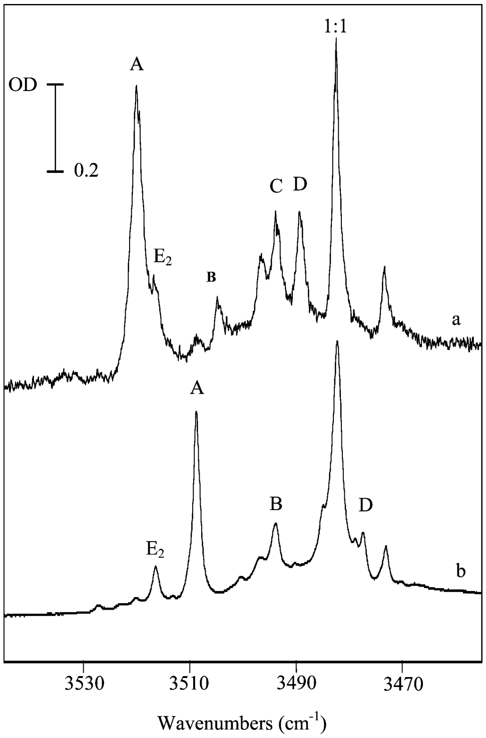

Figure 1. Effect of $CH_3{}^{16}OH$/$CH_3{}^{18}OH$ isotopic substitution in the PD νOH region of annealed ethanol/methanol/N_2 = 1/3/600 samples, a: $CH_3{}^{16}OH$, b: $CH_3{}^{18}OH$. E_2 = $(C_2H_5OH)_2$. A, B, C, D: $(CH_3OH)_2$.

indicates that the structure is type-I, the ethanol subunit acting as PD. Table 8 gathers the frequencies of the bands attributable to this species with their assignment based on those of homodimers $(CH_3OH)_2$[26] and $(C_2H_5OH)_2$.[10] All these bands which noticeably increase in intensity upon annealing decrease after a long exposure of the sample in the beam of the spectrometer, with concomitant appearance of bands at 3651, 3493.5, 1395, 1049, and 883 cm^{-1} ($CH_3{}^{16}OH$). The two low-frequency ones, assignable to νCO (methanol) and ν_sCCO (ethanol), respectively, characterize the PD character of the methanol molecule[5] and the PA character of ethanol.[9]

In Ar matrix, unlike N_2 matrix, there is no significant intensity increase of the bands of the heterodimer on annealing, which renders their identification still more difficult. In the region 3550−3490 cm^{-1} typical of dimeric hydrogen-bonded OH oscillators, the most favorable situation is obtained using $CH_3{}^{18}OH$ with C_2H_5OH in excess. Under these conditions the nearly complete absence of methanol dimer allows three bands at about 3513, 3506, and 3499 cm^{-1} to be assigned to C_2H_5OH:$CH_3{}^{18}OH$. When replacing $CH_3{}^{18}OH$ by $CH_3{}^{16}OH$ these bands are not observed, but a careful examination reveals the existence of two signals at about 3524 and 3510 cm^{-1}, respectively correlated to those at 3513 and 3499 cm^{-1} of C_2H_5OH:$CH_3{}^{18}OH$, with the expected 11 cm^{-1} isotopic blue shift. The counterpart of the signal at 3506 cm^{-1} for $CH_3{}^{18}OH$, expected at 3517 cm^{-1}, cannot be confidently assigned because of overlap with one band of $(CH_3OH)_2$.[13] In the free OH region, several weak bands between 3646 and 3642 cm^{-1}, not affected by isotopic substitution, are assignable to the heterodimer. Thus the ethanol:methanol dimer trapped in argon has a Type-II structure, the ethanol subunit acting as PA.

V. Monochromatic Irradiations

Selective irradiations were carried out at some of the νOH frequencies of the CH_3OH:H_2O and C_2H_5OH:H_2O dimers trapped in both N_2 and Ar matrices. Positive results were obtained only in N_2 matrix.

V.A. CH_3OH:H_2O in N_2 Matrix. Irradiations were carried out at the frequencies of the (methanol) OH-bonded oscillator, 3542, 3535, and 3531 cm^{-1}, corresponding respectively to sites α, γ, and δ. Significant effects, not limited to site interconversions, were observed in all cases. A typical example is shown in Figure 2 for irradiation at 3531 cm^{-1} (Type-I complex in site δ). The upper trace corresponds to the spectrum recorded before irradiation. Owing to the excess of water with respect to methanol, both $(H_2O)_2$ and CH_3OH:H_2O dimers are present but

TABLE 8: Vibrational Frequencies (cm^{-1}) of the Ethanol:Methanol (^{16}O and ^{18}O) Dimer Trapped in N_2 and in Ar at 4 K

N_2 matrix		Ar matrix		
^{16}O	^{18}O	^{16}O	^{18}O	assignment
3654.9 (24) 3647.0	3643.3 (16) 3635.5	3524.1[a] 3511.5 s 3509.9	3513.2 3506.3 s 3498.6	νOH methanol
3482.4 (100) 3473.3	3482.3 (100) 3473.1	3645.3 w 3642.4	3646.3 3645.5 w 3642.3	νOH ethanol
2851.8 (5.5)	2850.8 (4.5)	2837.1	2836.0	ν_sCH_3 methanol
1418.3 (15) 1274.4 (1.8)	1418.3 (12) 1274.2 (1.6)	1278.5 s	1278.5 s	δOH ethanol
1085.2 (16)	1094.5 1085.3 (15)			$rCH_3 + \nu_aCCO$ ethanol
1029.7 (28)	1002.8 (29)	1048.6 s 1046.3	1023.1 s 1020.6	νCO methanol
		1030.0 m	1030.0 m	$\nu_aCCO + rCH_3$ ethanol
886.3 (2.3)	886.3 (1.9)	883.2 w	883.2 w	ν_sCCO ethanol

[a] Overlap with the $(CH_3OH)_2$ δ band makes observation impossible.

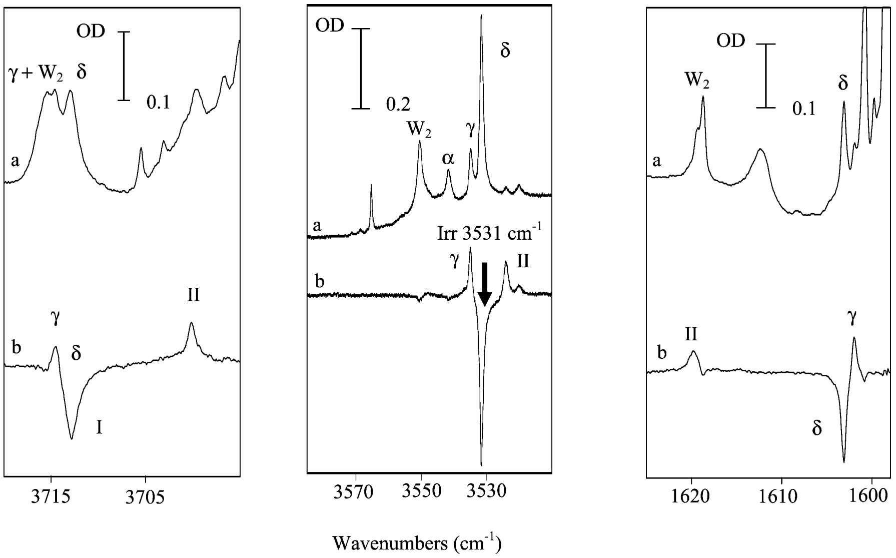

Figure 2. Effect of irradiation at 3532 cm^{-1} on a $CH_3OH/H_2O/N_2 = 1/3/600$ annealed sample. Recording temperature: 4 K. a: before irradiation. b: difference spectrum after 27 min irradiation. Laser power: 2 mW. W_2: $(H_2O)_2$; α, γ, δ: Type-I $CH_3OH{:}H_2O$ dimer (water PA); II: Type-II $CH_3OH{:}H_2O$ dimer (water PD).

$(CH_3OH)_2$, characterized by two main absorptions at 3520 and 3505 cm^{-1},[26] is nearly totally absent. The lower trace is the difference between spectra recorded after and before irradiation. The 3531 cm^{-1} signal is reduced to 10% of its initial value, being converted partly in type-I site γ (3535 cm^{-1} band), partly into a new species absorbing at 3524 and 3520 cm^{-1}. In the absorption domains of H_2O the decrease of the δ signals at 3713, 3627, and 1603 cm^{-1} is counterbalanced by the intensity increase of the γ ones and of those of the new species at 3700, 3524−3520, and 1620 cm^{-1}. The overall spectrum of this new species whose frequencies are close to that of the dimer trapped in argon[4] is reported in Table 9. The water frequencies are typical of H_2O acting as proton donor[22] whereas the νCO and δCOH frequencies, close to those of CH_3OH monomer, prove the proton acceptor character of this molecule. Thus the infrared-induced conversion of δ is:

$$CH_3OH\cdots OH_2\ (\delta) \xrightarrow{\nu_{irr}=3531} CH_3OH\cdots OH_2\ (\gamma) + HOH\cdots O(H)CH_3 \quad (1)$$

In a similar way irradiation at the νOH frequency of γ, 3534.9 cm^{-1}, leads to site exchange ($\gamma \rightarrow \delta$) and to the formation of Type-II complex characterized by the same bands as those observed for scheme (1). Thus one has:

$$CH_3OH\cdots OH_2,\ (\gamma) \xrightarrow{\nu_{irr}=3535} CH_3OH\cdots OH_2\ (\delta) + HOH\cdots O(H)CH_3 \quad (2)$$

Irradiation at 3542 cm^{-1}, νOH frequency of α, gives rise to somewhat different results, with the intensity decrease of the three Type-I α, γ, and δ dimers and the strong intensity increase of the band at 3524.0 cm^{-1} characterizing the Type-II species. Thus a Type-I → Type-II interconversion of the $CH_3OH{:}H_2O$ dimer is obtained upon irradiation at the νOH frequency of methanol whatever the nature of the trapping site of the dimer. Note that the bands observed after long sample exposure in the light beam of the spectrometer and reported in part IV are the same as those of Type-II dimer generated in monochromatic experiments. Thus interconversion also occurs, but to a smaller extent, with polychromatic infrared light. Once Type-II dimer has been generated, back conversion upon irradiation at its ν_1 frequency (3524 cm^{-1}) was examined. Positive effects were readily observed, with formation of both γ and δ Type-I species.

TABLE 9: Frequencies (cm^{-1}) of Type-I (δ) and Type-II $CH_3OH:H_2O$ Dimers (^{16}O for Both Molecules) Trapped in Solid N_2

modes[a]	Type-I (δ)[b]	Type-II
ν_3	3713.2 (44)	3699.8 (48)
ν_1	3627.2 (6)	3524.0 (100)
ν_2	1603.1 (24)	1619.8 (26)
νOH	3531.6 (100)	3661.2 (42)
νCH_3		
A′	2977.2 (8)	3010.0 (12)
A″	2946.2	
A′	2836.7 (12)	2848.1 (8.5)
δCH_3		
A′	1474.8 (1)	1473.7 (4.2)
A″	1463.2 (2.5)	1465.1 (2.5)
A′	1447.8 (1)	1449.9 (1.2)
δCOH	1391.0 (8)	1344.6 (17)
rCH_3	1101.0 (3)	1079.1
νCO	1048.1 (32)	1035.2 (46)

[a] ν_1, ν_2, ν_3 refer to the water vibrational modes. [b] Values taken from ref 5.

V. B. $C_2H_5OH:H_2O$ in N_2 Matrix. Two irradiation cycles at 3527 and 3645 cm^{-1} were successively carried out, leading to opposite interconversion processes.

Upon irradiation at 3527 cm^{-1}, νOH frequency of ethanol acting as proton donor, considerable spectral changes occur, as shown in Figure 3. On one hand the three bands of water at 3715, 3631, and 1603 cm^{-1} strongly decrease in intensity, with concomitant increase of signals close to 3700, 3500, and 1624 cm^{-1}, typical of water acting as PD. One thus concludes that Type-I → Type-II conversion occurs upon irradiation at 3527 cm^{-1}. On the other hand, in the fingerprint region of C_2H_5OH, three main bands at 1394, 1067, and 1058 cm^{-1} characterize this molecule after irradiation (Table 7).

Irradiation at 3645 cm^{-1} following that at 3527 cm^{-1} restores the initial situation. In a nitrogen matrix there occurs thus the photoconversion processes:

$$C_2H_5OH\cdots OH_2 \underset{\nu_{irr}=3645}{\overset{\nu_{irr}=3527}{\rightleftharpoons}} HOH\cdots O(H)C_2H_5$$

The Type-I → Type-II photoconversion also occurs upon exposure to the light beam of the spectrometer (conf. part IV), but this process is limited by back conversions (such as that occurring at 3645 cm^{-1}).

VI. Discussion

VI.A. Matrix-Dependent Structure of the Heterodimers. The donor or acceptor character of each subunit within the three heterodimers has been easily deduced from $^{16}O/^{18}O$ substitutions and, for those involving H_2O, from its ν_2 and ν_3 frequencies. Though less affected by hydrogen bonding than ν_1, these two modes experience a c.a. 20 cm^{-1} blue and red shift, respectively, from PA to PD. A remarkable matrix dependence, previously reported for the $CH_3OH:H_2O$ dimer,[4,5] is also observed for the two other heterodimers: the stable structure in argon corresponds to the metastable one in nitrogen. In Ar the smaller subunit plays the role of proton donor (Type-II structure), as expected since in a ROH molecule the basicity of the oxygen atom increases with the size of the alkyl group while the acidicity of the hydroxyl group decreases. This is in agreement with the results of ab initio calculations. In N_2, on the contrary, the structures are Type-I at equilibrium, but the Type-II forms are easily induced by vibrational excitation.

The stabilization of the high energy (Type-I) isomer in N_2 can be rationalized by considering cooperative effects[18] induced by the formation of very weak hydrogen bond between one hydroxyl group and one N_2 molecule acting as proton acceptor.[27] In the case of $ROH:H_2O$ dimers two $OH\cdots N_2$ interactions have to be taken into account:

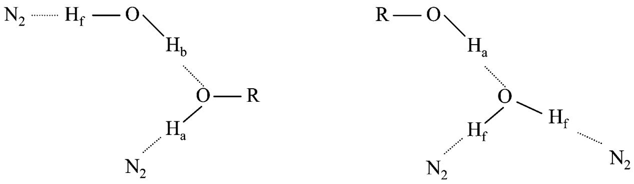

Type-II structure

Type-I structure

In Type-II structure the acid character of $O-H_b$ is weakened by the $N_2\cdots H_f$-O bonding, but the proton acceptor character of ROH is increased by the $N_2\cdots H_a$-O interaction. These two opposite effects can be considered as canceling each other. In

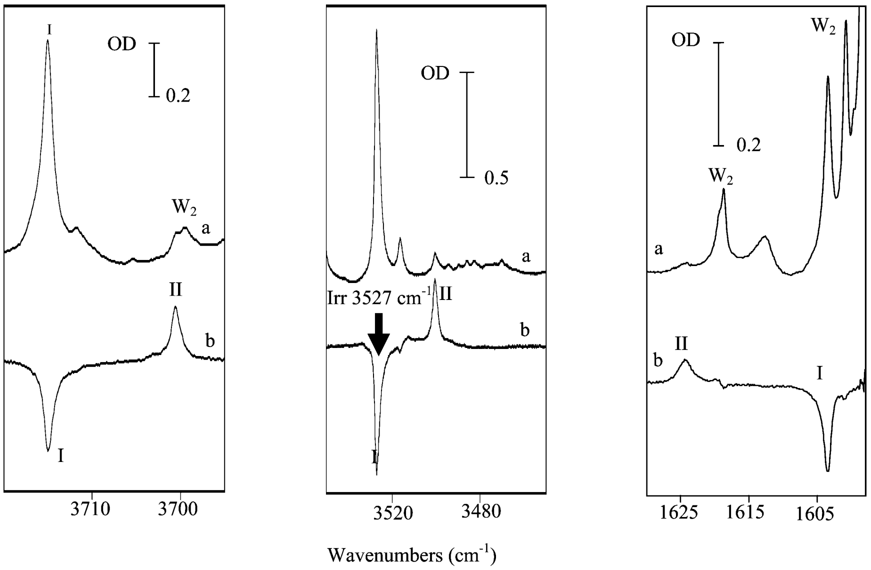

Figure 3. Effect irradiation at 3527 cm^{-1} on a $C_2H_5OH/H_2O/N_2$ = 1/3/600 annealed sample. Recording temperature: 4 K. a: before irradiation. b: difference spectrum after 35 min irradiation. Laser power: 1.5 mW. W_2: $(H_2O)_2$; I, II: Type-I, Type-II $C_2H_5OH:H_2O$ dimer (water PA, PD, respectively).

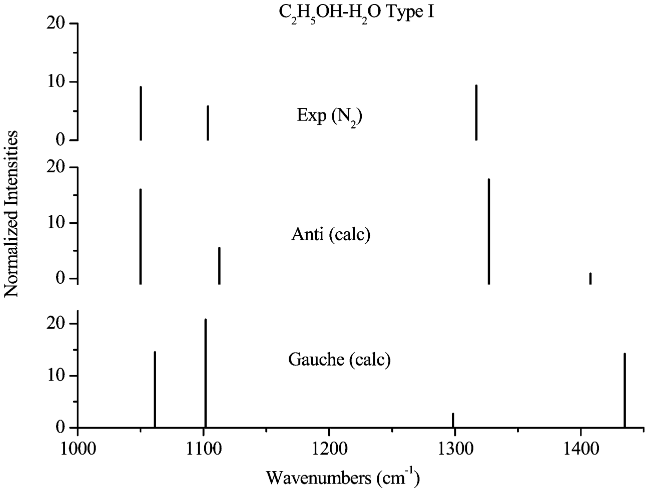

Figure 4. Bar spectra of Type-I C_2H_5OH:H_2O dimer. Lower traces: calculated for gauche and anti ethanol. Upper trace: observed spectrum in N_2 matrix. The intensities have been normalized with respect to νOH of ethanol ($I_{\nu OH} = 100$).

type-I structure the O−H_a•••O bonding is reinforced by the double donor role of the water (two Oh_f•••N_2 interactions). These contributions can overcome the energy difference between the two structures considered in vacuo, leading to the stabilization of Type-I.

For the ROH:R′OH pair (R = C_2H_5, R′ = CH_3) the type-II structure is more stable in vacuo because of a greater basicity and a weaker acidity of ethanol. The action of N_2 is stronger for Type-I than for Type-II (methanol being more acid), which reinforces more strongly the OH•••O bond and reverses the relative stability of the two isomers.

VI.B. Conformation of Ethanol in Type-I and Type-II Dimers. Following the method used for $(C_2H_5OH)_2$[9] it is possible to precise the conformation gauche or anti of the ethanol molecule engaged in the two heterodimers with water or methanol by comparing its main absorptions in the fingerprint region (1450−1000 cm^{-1}) with the results of our DFT calculations.

In Type-I dimer the main absorptions of PD ethanol are calculated at about 1330, 1110, 1050 and 1430, 1100, 1060 cm^{-1} for the anti and gauche forms, respectively. Figure 4 compares the calculated bar spectra of anti and gauche ethanol in Type-I C_2H_5OH:H_2O dimer with the observed one in N_2 matrix. A good agreement is obtained for the anti form, characterized by a strong band around 1320 cm^{-1}, assignable to δOH, whose counterpart for the gauche form is calculated at much higher frequency, around 1430 cm^{-1}. For Type-I C_2H_5OH:CH_3OH dimer identified in N_2 the main absorptions of ethanol are measured at 1418 and 1085 cm^{-1} with comparable intensities; this result is compatible with a gauche structure.

In Type-II dimer the main absorptions of PA ethanol are calculated at about 1270, 1090, 1035 and 1420, 1070, 1050 cm^{-1} for the anti and gauche forms, respectively. The bar spectra in Figure 5 clearly show that the observed spectrum for C_2H_5OH:H_2O in N_2 correctly fits the calculated gauche form. In Ar matrix three bands at 1028.7, 1083.7, and ca. 1270 cm^{-1} are confidently assigned to this dimer. The first one is remarkably close to the signal at 1027.4 cm^{-1} observed for $(C_2H_5OH)_2$ trapped in argon and assigned to PA in its anti form.[10] Accordingly we suggest that in the Type-II C_2H_5OH:H_2O dimer trapped in Ar, the ethanol subunit is in anti conformation. For Type-II C_2H_5OH:CH_3OH dimer trapped in Ar, the presence of two main bands at 1030 and 1278 cm^{-1} unambiguously characterizes as anti conformation. Table 10 gathers the conformational dependence of ethanol acting as PA or PD as a function of the partner and of the matrix. For PA ethanol, it appears that the conformation is that observed for the monomer[9] and at variance for Ar and N_2.

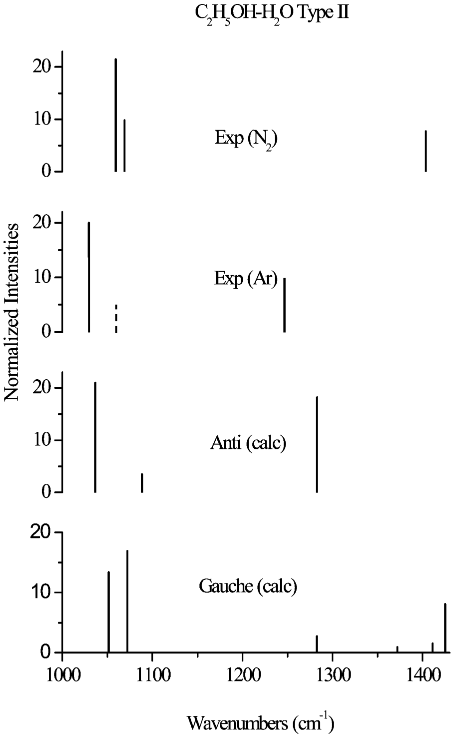

Figure 5. Bar spectra of C_2H_5OH in Type-II C_2H_5OH:H_2O dimer. Lower traces: calculated for gauche and anti forms. Upper traces: observed in Ar and N_2 matrices. The intensities have been normalized with respect to νOH of methanol ($I_{\nu OH} = 100$).

TABLE 10: Conformation of Ethanol Acting as PA or PD in C_2H_5OH:ROH Dimers (R = H, CH_3, C_2H_5) Trapped in Ar or N_2 Matrix[a]

	PA C_2H_5OH		PD C_2H_5OH	
	Ar	N_2	Ar	N_2
H_2O	anti	gauche	n.o.	anti
CH_3OH	anti	n.o.	n.o.	gauche
C_2H_5OH[b]	anti	gauche	anti	anti

[a] Note that the stable forms of ethanol monomer are anti and gauche in Ar and N_2, respectively. n.o. = not observed. [b] Reference 10. Forms C and α in Ar and N_2, respectively, which are the most abundant.

VI.C. Hydrogen Bond Strength and νOH Frequency in the ROH:R′OH Dimers. The complete set of spectral data on homo and heterodimers ROH:R′OH (R, R′ = H, CH_3, C_2H_5) trapped in Ar and N_2 allows a discussion of the hydrogen bond strength as a function of R and R′ to be developed on the basis of the νOH frequency of the proton donor molecule. These frequencies are reported in Table 11. In case of band splitting due to multiple trapping sites a mean value has been reported. For an easier comparison with the theoretical results, the frequency shifts -$\Delta\nu = \nu OH_{free} - \nu OH_{PD}$ are also reported. In the case of water νOH_{free} corresponds to the value measured for HDO (3687 and 3682 cm^{-1} in Ar[20] and N_2,[16] respectively) in order to get rid of the coupling between the OH oscillators of the reference molecule. However one has to keep in mind that there remains some residual coupling, of the order of 10 cm^{-1}, between free and bound OH oscillators of the water molecule acting as PD. Table 11 has to be read vertically and horizontally. In a column, PD is fixed and the basicity of PA

TABLE 11: Correlation between νOH Frequencies and Frequency Shifts $\Delta\nu = \nu OH_b - \nu OH_{Free}$ for PD Units in ROH:R′OH Homo and Heterodimers (R, R′ = H, CH_3, C_2H_5). All values in cm^{-1}

	H_2O[a]			CH_3OH			C_2H_5OH[h]		
R of PA/PD	Ar	N_2	calcd	Ar	N_2	calcd	Ar	N_2	calcd
H[a]									
ν	3574[b]	3550	3705[c]	n.o.	3536[d]	3727	n.o.	3527(A)	3724(A)
$-\Delta\nu$	113	132	169		128	124		126	123
CH_3									
ν	3539[e]	3524	3674	3530[f]	3504[g]	3695	n.o.	3482(G)	3693(A)
$-\Delta\nu$	148	158	200	136	160	156		167	154
C_2H_5[h]									
ν	3534(A)	3500(G)	3666(A)	3516(A)[i]	3493(G)	3685 (A)	3530[j](A,A)	3500[j](G,A)	3684(A,A)
$-\Delta\nu$	153	182	208	151	171	166	126	152	163

[a] For H_2O $\nu OH_{free} = \nu_3$(HDO) = 3682 (N_2) [22], 3687 (Ar) [24], and 3874 cm^{-1} (calcd). [b] Reference 24. [c] Reference 12. [d] Reference 5. Mean frequency of four components. [e] Reference 4. Mean frequency of two components. [f] Reference 13. Mean frequency of four components. [g] *J. Chim. Phys*. **1993**, *90*, 1703. Mean frequency of five components. [h] Form anti (A) or gauche (G) specified. For $(C_2H_5OH)_2$ specification in the order PA, PD. [i] This work. Mean frequency of four components. [j] Reference 10. Mean frequency of several components.

increases downward. As a consequence $-\Delta\nu$ is expected to increase; this is correctly predicted theoretically and observed in both matrices, with the exception of C_2H_5OH acting as PD in N_2 matrix, for which a much larger shift is observed for PA = CH_3OH than for PA = C_2H_5OH. Such an inversion cannot be explained by a conformational change, the less so as the νOH frequency is 3516 cm^{-1} for $(C_2H_5OH)_2$ in its predominant gauche conformation,[10] the same as that observed for C_2H_5-OH···OH(CH_3). If one considers now one line of Table 11, the acid character of PD decreases from left to right so that at fixed PA one may expect a correlated decrease of $-\Delta\nu$. This is well verified theoretically and also for the incomplete set of data in Ar. In N_2 there is a large discrepancy for PA = CH_3OH since the largest $-\Delta\nu$ value is observed for PD = C_2H_5OH. This value was also source of problem in the analysis of the C_2H_5OH···O(H)R/N_2 column. Since the assignment based on $CH_3{}^{16}OH$/$CH_3{}^{18}OH$ isotopic substitution seems unquestionable, we can only suggest a specific constraint of the N_2 matrix reinforcing the hydrogen bond. It would be useful to perform experiments with larger PD molecules (C_3H_7OH, etc.) to confirm the classification.

VII. Conclusion

This work generalizes two kinds of observations previously reported for homodimers $(ROH)_2$, R = H, CH_3, C_2H_5, and for the CH_3OH:H_2O heterodimer: the matrix-dependent structure and the sensitivity to infrared light of hydrogen-bonded aggregates. The heterodimers, which are calculated to be more stable in their Type-II structure (the smaller subunit acting as proton donor), keep that structure in argon matrix but exchange the role of the partners in solid nitrogen. This interchange can be understood by considering the existence of hydrogen bonding between the free OH oscillator(s) (one bond for R and R′ ≠ H_2O, two for R or R′ = H_2O) and N_2 molecule(s). Indeed the main OH···O bond is reinforced or weakened according to whether the OH oscillator involved in the OH···N_2 interaction belongs to the proton acceptor or to the proton donor molecule. Nevertheless the stable Type-I structure in solid N_2 is easily converted into the Type-II one by vibrational excitation induced by polychromatic and, to a larger extent, by selective monochromatic infrared irradiation. This photoisomerization, which stems from the well-known predissociation process at the origin of the photodepletion spectroscopy in the gas phase, is only observed in solid N_2 because the lifetime of the metastable species is compatible with the duration of spectral acquisition for temperatures lower than ca. 15 K. In solid argon this lifetime is probably drastically reduced because of the decrease of the steric constrainst. Fast acquisition and/or temperatures lower than 4 K should be required for its observation.

References and Notes

(1) Buck, U.; Huisken, F. *Chem. Rev.* **2000**, *100*, 3863.

(2) Huisken, F.; Stemmler, M. *Chem. Phys. Lett.* **1991**, *180*, 332.

(3) Stockman, P. A.; Blake, G. A.; Lovas, F. J.; Suenram, R. D. *J. Chem. Phys*. **1997**, *107*, 3782.

(4) Bakkas, N.; Bouteiller, Y.; Loutellier A.; Perchard, J. P.; Racine, S. *Chem. Phys. Lett*. **1995**, *232*, 90.

(5) Bakkas, N.; Bouteiller, Y.; Loutellier, A.; Perchard, J. P.; Racine, S. *J. Chem. Phys*. **1993**, *99*, 3335.

(6) Coussan, S.; Bouteiller, Y.; Perchard, J. P.; Brenner, V.; Millié, P.; Zheng, W. Q.; Talbot, F. *J. Chem. Phys.* **1999**, *110*, 10046.

(7) Coussan, S.; Brenner, V.; Perchard, J. P.; Zheng W. Q. *J. Chem. Phys*. **2000**, *113*, 8059.

(8) Heikkilä, A.; Pettersson, M.; Lundell, J.; Khriachtchev, L.; Räsänen, M. *J. Phys. Chem. A* **1999**, *103*, 2945.

(9) Coussan, S.; Bouteiller, Y.; Perchard, J. P.; Zheng, W. Q. *J. Phys. Chem. A* **1998**, *102*, 5789.

(10) Coussan, S.; Alikhani, M. E.; Perchard, J. P.; Zheng, W. Q. *J. Phys. Chem. A* **2000**, *104*, 5475.

(11) Dyczmons, V. *J. Phys. Chem. A* **2004**, *108*, 2080.

(12) Coussan, S.; Roubin, P.; Perchard, J. P. *Chem. Phys*., in preparation.

(13) Coussan, S.; Bouteiller, Y.; Loutellier, A.; Perchard, J. P.; Racine, S.; Peremans, A.; Zheng, W. Q.; Tadjeddine, A. *Chem. Phys*. **1997**, *219*, 221.

(14) Frish, M. J., et al., GAUSSIAN, Revision A9; Gaussian Inc., Pittsburgh, PA, 1998.

(15) Becke, A. D. *J. Chem. Phys.* **1993**, *98*, 5648.

(16) Lee, C.; Wang, W.; Parr, R. G. *Phys. Rev. B* **1998**, *37*, 785.

(17) Boys, S. F.; Bernardi, F. *Mol. Phys*. **1970**, *19*, 553.

(18) Mó, O.; Yáñez, M.; Elguero, J. *J. Chem. Phys*. **1992**, *97*, 6628.

(19) Mó, O.; Yáñez, M.; Elguero, J. *J. Mol. Struct*. **1994**, *314*, 73.

(20) González, L.; Mó, O.; Yáñez, M. *J. Chem. Phys*. **1998**, *109*, 139.

(21) Peeters, D.; Leroy, G. *J. Mol. Struct. (THEOCHEM)* **1994**, *314*, 39.

(22) Fredin, L.; Nelander, B.; Ribbegard, G. *J. Chem. Phys.* **1977**, *66*, 4065.

(23) Perchard, J. P. *Chem. Phys.* **2001**, *266*, 109.

(24) Ayers, G. P.; Pullin, A. D. E. *Spectrochim. Acta* **1976**, *32* A, 1629.

(25) Perchard, J. P. *Chem. Phys*. **2001**, *273*, 217.

(26) Coussan, S.; Loutellier, A.; Perchard, J. P.; Racine, S.; Peremans, A.; Tadjeddine, A.; Zheng, W. Q. *Chem. Phys*. **1997**, *223*, 279.

(27) Coussan, S.; Loutellier, A.; Perchard, J. P.; Racine, S.; Bouteiller, Y. *J. Mol. Struct*. **1998**, *471*, 37.